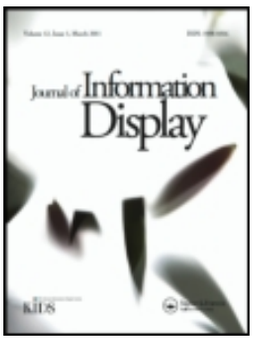

Journal of Information Display

ISSN: 1598-0316 (Print) 2158-1606 (Online) Journal homepage: https://www.tandfonline.com/loi/tjid20

Capillary force lithographic patterning of a thermoplastic polymer layer for control of azimuthal anchoring in liquid crystal alignment

Hak-Rin Kim , Min-Soo Shin , Kwang-Soo Bae & Jae-Hoon Kim

To cite this article: Hak-Rin Kim , Min-Soo Shin , Kwang-Soo Bae & Jae-Hoon Kim (2008) Capillary force lithographic patterning of a thermoplastic polymer layer for control of azimuthal anchoring in liquid crystal alignment, Journal of Information Display, 9:1, 14-19, DOI: 10.1080/15980316.2008.9652046

To link to this article: https://doi.org/10.1080/15980316.2008.9652046

Capillary Force Lithographic Patterning of a Thermoplastic Polymer Layer for Control of Azimuthal Anchoring in Liquid Crystal Alignment

Hak-Rin Kim[*a], Min-Soo Shin[b], Kwang-Soo Bae[**b], and Jae-Hoon Kim[*b,c]**

Abstract

We demonstrated the capillary force lithography (CFL) method for controlling the azimuthal anchoring energy of a liquid crystal (LC) alignment layer. When a thermoplastic polymer film is heated to over the glass transition temperature, the melted polymer is filled into the mold structure by the capillary action and the aspect ratio of the pattern is determined by the dewetting time of the CFL process. Here, the proposed method showed that the azimuthal anchoring energy of the LC alignment layer could be simply controlled by the surface relief patterns which were determined by the dewetting times during the CFL patterning.

Keywords : Capillary force lithography, Azimuthal anchoring, Liquid crystal, PMMA(polymethylmethacrylate)

1. Introduction

In liquid crystal displays (LCDs) and other liquid crystal (LC)-based devices, the surface anchoring properties of LC molecules on an LC alignment layer is one of the most important factors determining their electro-optic properties (EO). The physical model of LC anchoring is decomposed into two anchoring energy terms of azimuthal anchoring and polar anchoring. The LC anchoring mechanisms on surfaces are explained by the topological effects on a groove surface [1] and the chemophysical effects on a polymer surface with aligned polymer chains [2]. Between the two anchoring mechanisms, the topological effects explain why the LC molecules align along the groove direction through the minimization of the elastic strain energy of LC molecules on the surface relief structure, which was first examined by Berreman [1]. According to the Berreman's derivation, the azimuthal LC anchoring energy of the solid groove surface is determined by the aspect ratio of the periodic groove structure. Until now, several surface modification methods have been proposed to make micro-grating structures and to control the azimuthal anchoring energy.

However, conventional surface modification methods - such as laser etching [3] or ablation of polymer layers, stamping for morphological changes [4], formation of surface relief structure on azo-dye doped polymer films, photolithographic methods [5, 6], and AFM scribing [7-9] - are not convenient for fabrication and some are inadequate for mass-production. Most importantly, it is difficult to control the aspect ratio, which is essential in azimuthal anchoring control, when these conventional approaches are used.

In this work, we introduce a capillary force lithographic patterning method [10-12] which can easily control the aspect ratio of micro-grating surface patterns. The proposed method shows the anchoring energy of an LC alignment layer can be controlled only by varying the dewetting time of a thermoplastic polymer layer preserving conformal contact of an elastomeric mold during the capillary force lithography (CFL) process. Here, we discuss the topological surface modification produced by the CFL patterning and resulting azimuthal LC anchoring control with a thermoplastic polymer of polymethlymethacrylate (PMMA: Sigma-Aldrich Co.).

Manuscript received January 15, 2008; accepted for publication March 25, 2008.
This research was supported by Kyungpook National University Research Fund, 2007.
* Member, KIDS; ** Student Member, KIDS
Corresponding Author : Jae-Hoon Kim
[a]School of Electrical Engineering and Computer Science, Kyungpook National University, Daegu 702-701 , Korea
[b]Department of Information Display Engineering, Hanyang University, Seoul 133-791, Korea
[c]Department of Electronics and Computer Engineering, Hanyang University Seoul 133-791, Korea
E-mail : jhoon@hanyang.ac.kr
Tel : 81-02-2220-0343 **Fax** : 81-02-2298-0345

2. CFL patterning of PMMA layer

Fig. 1 shows our CFL patterning process for producing the periodic surface patterns. First, a thermoplastic polymer in solvent was spin-coated on a glass substrate and the polymer layer was cured. In our experiment, we used PMMA as a thermoplastic polymer for CFL patterning. On the PMMA film, we put an elastomeric mold preserving the conformal contact without pressure. Then, the substrates were heated above the glass transition temperature (T_g) of PMMA and the PMMA film were melted. During this annealing process, the mold structure sank down to the PMMA layer and the melted polymer was filled into the mold structure by the capillary action [11,12]. After cooling down to room temperature, the mold was carefully removed and the patterned PMMA structure was obtained. In the final structure, the aspect ratio and the morphology of the pattern were determined by the dewetting time, or the capillary filling time, of the CFL patterning and the wetting properties between the melted polymer and the mold surface [11,12].

In selecting patterning materials, T_g of a thermoplastic polymer is important in two aspects. To minimize the thermal expansion of the mold structure and to avoid distortion

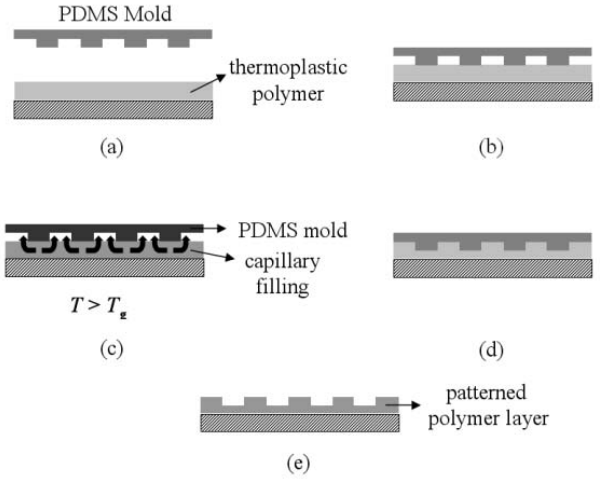

Fig. 1. The schematic diagram showing the capillary lithographic patterning process with a thermoplastic polymer : (a) preparing an elastomeric mold, spin-coating and then curing an thermoplastic polymer, (b) contacting the mold structure on the thermoplastic polymer layer without pressure, (c) schematics of capillary filing of the melted thermoplastic polymer into the mold structure over the glass transition temperature (T_g) of the thermoplastic polymer, (d) the structure after the dewetting process, (e) the patterned polymer structure after removing the mold.

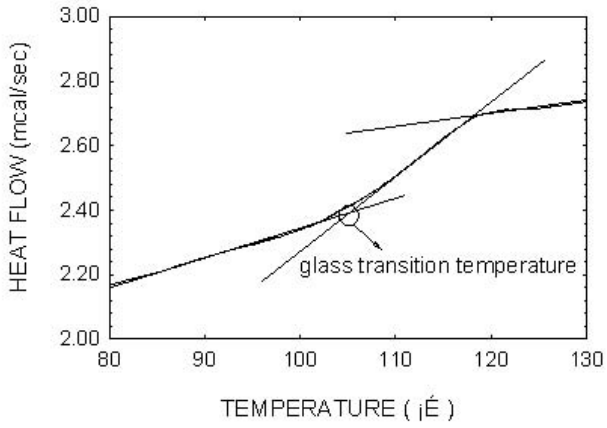

Fig. 2. DSC result of PMMA (polymethlymethacrylate).

of the mold pattern, T_g of the patterning material should not be too high. However, T_g should be over the nematic-isotropic phase transition temperature (T_{NI}) of LCs used in the experiment for obtaining uniform LC alignment. In our experiment, T_g of the PMMA was about 106 ^oC, which was measured by DSC (Differential Scanning Calorimetry : TA instrument) as shown in Fig. 2. The dewetting-induced patterning of the PMMA was executed at 130 ^oC. As an LC, E7 (T_{NI} =60.5 ^oC) from E. Merck was used.

The PMMA has another merit in investigating topological effects on LC anchoring since the PMMA acts as a surface gliding layer. There is only very weak chemophysical interaction between the PMMA surface and LC molecules as shown in the chemical structure of Fig. 3(a). The effect of the PMMA chain ordering on LC anchoring was checked by observing the LC texture (Fig. 3(b)) through the polarizing optical microscope (POM), where the LC was filled at $T>T_{NI}$ between the antiparallel-rubbed PMMA layers. The surface memory effect induced by the surface wetting on LC anchoring were also checked by preparing the LC cell having a directional ordering by the flow effects and then heating over T_{NI}. The schlieren textures of Figs. 3(b) and (d) mean that we can neglect the chemophysical effect on the LC anchoring in our PMMA.

Figs. 4(a) and (b) show the SEM images of the patterned SiO_2 master substrate and the PDMS mold substrate, respectively. The periodicity (λ) and the height (h) of the groove pattern in the master substrate was λ = 4 μm and h =900 nm, respectively. The PDMS mold was replicated from the master substrate and the periodicity of the PDMS pattern was also λ = 4 μm. With the PDMS mold, we patterned the PMMA layer with the CFL method by varying

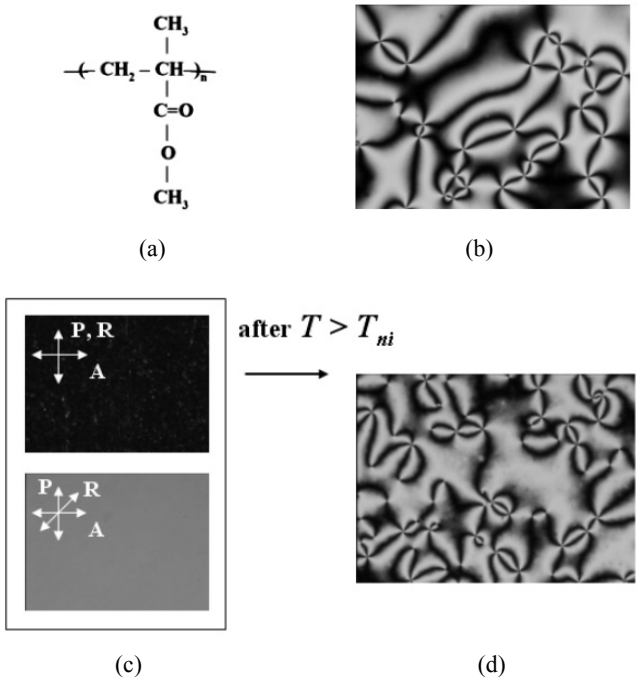

(a) (b)

(c) (d)

Fig. 3. (a) Chemical structure of PMMA, (b) the polarizing optical microscopic image (POM) of the LC cell, when the LCs are filled in an isotropic phase between the anti-parallel rubbed PMMA layers, (c) the POM image of the LC cell, when the LCs are filled in a nematic phase and the LCs are ordered by the flow effects, (d) the POM image of the LC cell obtained after the cell of Fig. 3(c) is heated over the nematic-isotropic phase transition temperature (T_{NI}) of the LC and then cooled down to room temperature.

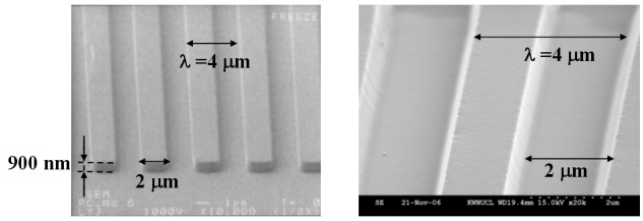

(a) (b)

Fig. 4. The SEM images of (a) the patterned SiO_2 master substrate and (b) the PDMS mold substrate replicated from the master substrate.

the dewetting time (t_d). The elastomeric PDMS mold could be re-used several times without severe damage of the mold pattern. The AFM images in Fig. 5 show the surface profiles of the patterned PMMA layer obtained at different dewetting times. The periodicities of the PMMA patterns were the same for all samples. However, the heights (2u) of the patterns increased as t_d increased, which means that the aspect ratio of the PMMA pattern was increased as t_d increased.

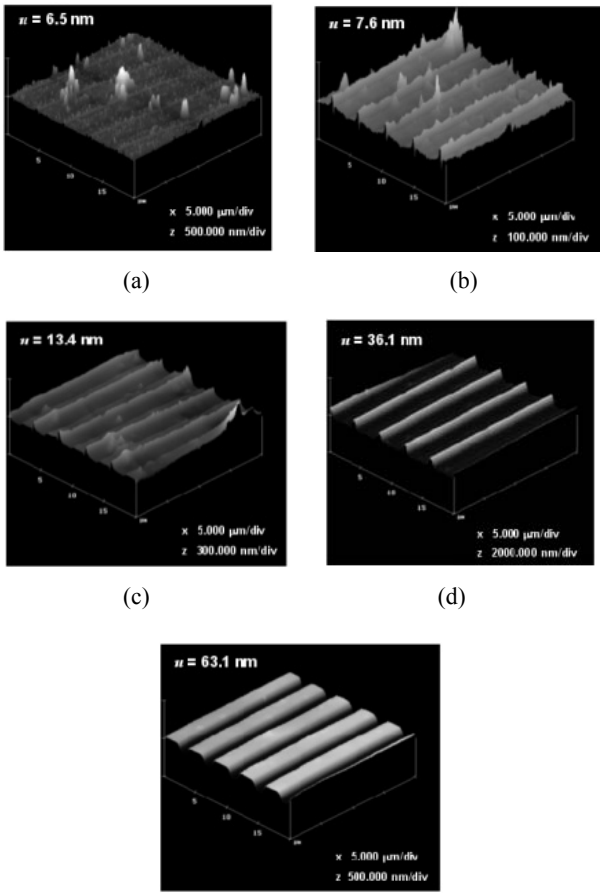

(a) (b)

(c) (d)

(e)

Fig. 5. The AFM images showing the surface profiles of the patterned PMMA layer obtained at different dewetting times (t_d) : (a) t_d = 1 min, (b) t_d = 3 min, (c) t_d = 7 min, (d) t_d = 30 min, (e) t_d = 60 min.

3. Control of azimuthal anchoring by CFL patterning

The azimuthal anchoring energy (W_ϕ) of the patterned PMMA surface was checked by preparing twisted nematic cells as shown in Fig. 6. As the other substrate, the unidirectionally rubbed polyimide (PI) layer was used. The rubbed PI surface was assumed as infinite anchoring surface along the rubbing direction. The azimuthal anchoring energy can be obtained as follows [13],

$$W_\phi = \frac{2K_{22}\phi}{d \sin 2\phi} \tag{1}$$

where K_{22}, ϕ, and d are the twist elastic constant of the LC, the twist angle of the LC structure, and d is the cell gap, respectively. K_{22} of E7 is $6.5*10^{-12}$ N. The cell gaps measured in our samples are listed in Table 1.

Table 1. The cell parameters prepared at different dewetting patterns of PMMA layers.

Dewetting time of PMMA	Cell gap (μm)	Height of Pattern 2u (nm)	Rotation Angle of Polarization γ (deg)	Twist Angle of LC Cell ϕ (deg)	Azimuthal Anchoring Energy W_ϕ (10^{-6} J/m^2)
1 min	10.9	13.00	7.4°	7.8°	0.58
3 min	11.1	15.19	24.3°	25.3°	0.64
7 min	10.7	26.87	41.1°	42.4°	0.87
30 min	11.4	72.14	75.3°	77.3°	3.49
60 min	10.4	126.23	80.4°	81.5°	6.00

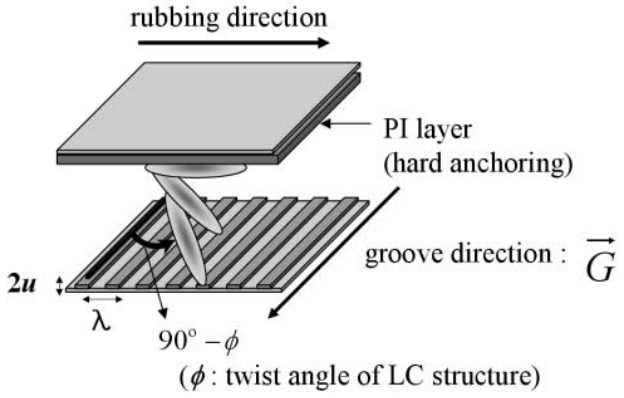

Fig. 6. The schematic diagram of the LC cell structure for measuring the azimuthal anchoring energy of the patterned PMMA layer.

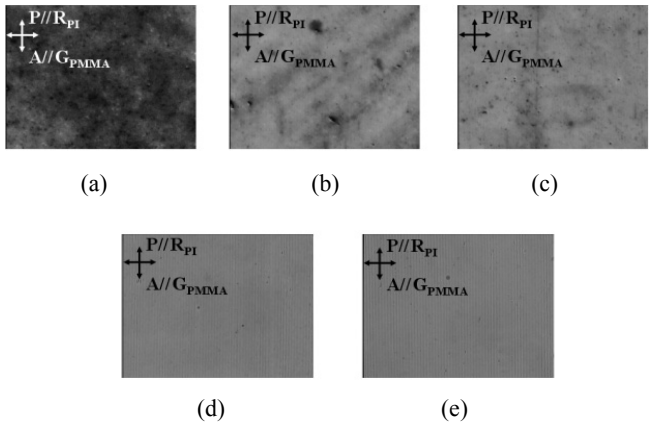

Fig. 7. The POM images of the LC textures, where the LC cells are assembled with the cell structure shown in Fig. 6. The dewetting times of the patterned PMMA layers are (a) t_d = 1 min, (b) t_d = 3 min, (c) t_d = 7 min, (d) t_d = 30 min, (e) t_d = 60 min.

Fig. 7 shows the POM images of the LC texture, where the LCs were assembled with the cell structure shown in Fig. 6. When the dewetting times were not sufficient to form the pattern with the high aspect ratio, the LC textures were not uniform as shown in Figs. 7 (a), (b), and (c). Whereas, Figs. 7(d) and (e) show the uniform LC textures, which means that the PMMA patterns made by dewetting times of t_d=30 min and t_d=60 min have relatively high azimuthal anchoring energies.

Once we know the exact twist angle of the LC structure, we can derive the azimuthal anchoring energy of the patterned PMMA surface. To obtain twist angle of each LC cell, we irradiated the linearly polarized probe beam onto the rubbed PI surface of the LC cell (Fig. 6), where the incident polarization was parallel to the rubbing direction of the PI. Then, we measured the polarization state of the output beam by rotating an analyzer. Here, we used He-Ne laser as the probe beam. Fig. 8 shows the normalized light transmittances of the LC cells measured by rotating the transmission axis of the analyzer with respect to the rubbing direction of the PI layer. By fitting the results of Fig. 8 with the Malus' law, we obtained the rotation angles of the polarizations at each sample, which are summarized in Table 1. The twist angle (ϕ) of the LC structure at each sample can also be obtained by fitting the results of Fig. 8 with the following equation derived from the Jones calculus.

$$T = \left\{\cos(\phi-\theta_a)\cos\beta - \frac{1}{\sqrt{1+\alpha^2}}\sin(\phi-\theta_a)\sin\beta\right\}^2 + \frac{\alpha^2}{1+\alpha^2}\cos^2(\phi-\theta_a)\sin^2\beta, \quad (2)$$

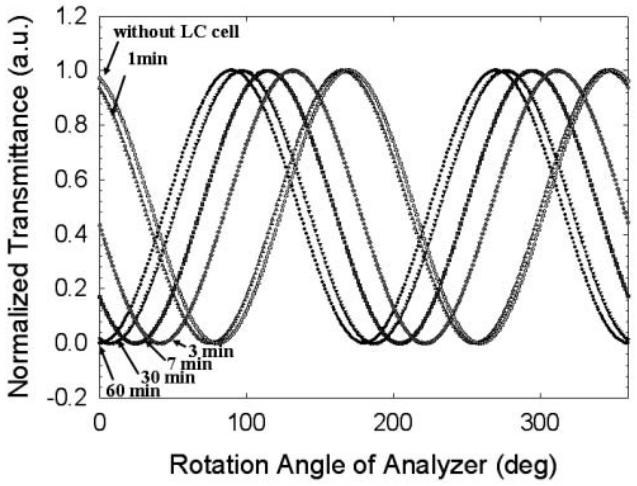

Fig. 8. The normalized light transmittances of the LC cells measured by rotating the transmission axis of the analyzer with respect to the transmission axis of the polarizer.

where $\alpha = \pi d\Delta n / \phi\lambda$, $\beta = \phi\sqrt{1+\alpha^2}$. θ_a and Δn are the analyzer angle and the birefringence of the LC, respectively. Here, Δn of E7 was about 0.22. ϕ's are summarized in Table 1.

From Eq. (1) and the fitted ϕ's, the azimuthal anchoring energy at each PMMA surface was obtained and the results are summarized in Table 1 and plotted in Fig. 9 (a). Fig. 9(a) shows that W_ϕ increased as t_d increased. When t_d > 10 min, W_ϕ became order of 10^{-6} J/m^2. These results mean that we can produce the azimuthal LC anchoring on the gliding polymer surface within tens of minutes and the amount of the anchoring energy can be also controlled with single process parameter. According to the Berreman theory, W_ϕ is proportional to u^2/λ^3, where u and λ are the amplitude and the periodicity of the periodic surface grating. With the parameters listed in Table 1, u^2/λ^3 's are obtained and plotted with W_ϕ, as shown in Fig. 9(b). Fig. 9(b) shows the PMMA pattern obtained at t_d = 60 min does not follow the Berreman equation, $W_\phi \propto u^2/\lambda^3$ [1]. The reason is that the surface topology of the PMMA pattern is not a sinusoidal pattern at t_d = 60 min. This means that we have to consider the shape of the mold pattern as well as the wetting properties of the melted polymer on the mold surface if we want to control the azimuthal anchoring energy of the thermoplastic polymer surface having a predictable as well as a sufficient value.

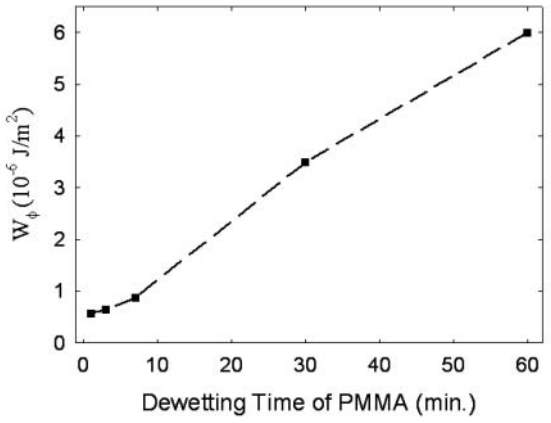

(a)

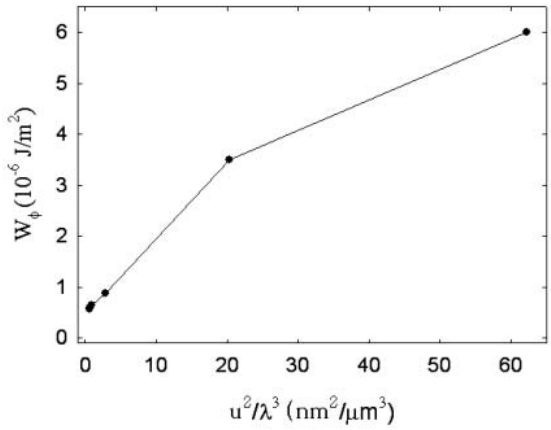

(b)

Fig. 9. (a) W_ϕ depending on the dewetting time of the PMMA patterns, (b) W_ϕ of the patterned PMMA layer depending on the surface groove profile (u^2/λ^3).

4. Conclusions

We have demonstrated that the azimuthal LC anchoring energy of a thermoplastic polymer surface can be easily controlled by varying the dewetting time during CFL patterning. We found that the aspect ratio increases as the dewetting time increases. Since the aspect ration of the surface grating pattern determines the LC anchoring energy due to the topological effects, we can expect and design the amount of the azimuthal anchoring energy. The experimental results show that we can get sufficient anchoring energies in obtaining uniform LC texture within tens of minutes with single soft-lithographic patterning process. Although the presented patterns are simple periodic line patterns, we can modify the grating directions and the aspect ratio of the grating pattern arbitrarily only by designing and changing

the elastomeric mold structure. Therefore, it is concluded that the proposed method can be used to develop complex LC geometries induced by the patterned surface can be easily obtained and new LC mode.

References

[1] D. W. Berreman, *Phys. Rev. Lett.* **28**, 1683 (1972).

[2] J. M. Geary, J. W. Goodby, A. R. Kmetz, and J. S. Patel, *J. Appl. Phys.* **62**, 4100 (1987).

[3] C. J. Newsome, M. O'Neill, R. J. Farley, and G. P. Bryan-Brown, *Appl. Phys. Lett.* **72**, 2078 (1998).

[4] E. S. Lee, P. Vetter, T. Miyashita, T. Uchida, M. Kino, M. Abe, and K. Sugawara, *Jpn. J. Appl. Phys. Part 2* **32**, L1436 (1993).

[5] Y. Kawata, K. Takatoh, M. Hasegawa, and M. Sakamoto, *Liq. Cryst.* **16**, 1027 (1994).

[6] G. P. Bryan-Brown, J. R. Sambles, and K. R. Welford, *J. Appl. Phys.* **73**, 3603 (1993).

[7] J.- H. Kim, M. Yoneya, and H. Yokoyama, *Nature* **420**, 159 (2002).

[8] B. Wen, M. P. Mahajan, C. Rosenblatt, *Appl. Phys. Lett.* **76**, 1240 (2000).

[9] A. J. Pidduck, S. D. Haslam, G. P. Bryan-Brown, R. Bannister, and I. D. Kitely, *Appl. Phys. Lett.* **71**, 2907 (1997).

[10] . Xia and G. M. Whitesides, *Angew. Chem. Int. Ed.* **37**, 550 (1998).

[11] C. M. Bruinink, M. Peter, M. de Boer, L. Kuipers, J. Huskens, and D. N. Reinhoudt, *Adv. Mater.* **16**, 1086 (2004).

[12] K. Y. Suh, Y. S. Kim, and H. H. Lee, *Adv. Mater.* **13**, 1386 (2001).

[13] G. P. Bryan-Brown and I. C. Sage, *Liq. Cryst.* **20**, 825 (1996).